# Large invisible carbon sink potential of global clay minerals to mitigate climate change

**Huipeng Xi**
Institute of Geochemistry, Chinese Academy of Sciences
**Xiaoyong Bai** (baixiaoyong@vip.skleg.cn)
Institute of Geochemistry, Chinese Academy of Sciences
**Luhua Wu**
Institute of Geochemistry, Chinese Academy of Sciences
**Chaojun Li**
Institute of Geochemistry, Chinese Academy of Sciences
**Huan Chen**
State Key Laboratory of Environmental Geochemistry, Institute of Geochemistry, Chinese Academy of Sciences

---

**Article**

**Keywords:** Chemical weathering, Carbon sink, Soil minerals, Climate change, 24 carbon budget

**Posted Date:** November 17th, 2021

**DOI:** https://doi.org/10.21203/rs.3.rs-1057950/v1



---

# Large invisible carbon sink potential of global clay minerals to mitigate climate change

**Abstract:** The chemical weathering of clay minerals widely distributed in the soil have great potential of carbon sink (CS), but the magnitude and influence mechanisms of this CS are unclear. Here we analyse recent changes in five major clay minerals (chlorite, smectite, mica, illite, and vermiculite) carbon sink and its driving factors, using a process-based model (PROFILE) and satellite data assimilation. We show that magnitude of CS in five major clay minerals is about 0.11 Pg C $yr^{-1}$ from 0 to 2m depth of soil, which is one third of CS in rocks and also may be mainly responsible for the world's missing carbon sink. According to our simulations, the linear trend of CS during 1970-2018 showing that CS in 56% of the world increasing significantly, although the intensification of CS cannot be explained by soil moisture (SM) or soil temperature (STMP) alone, they are the dominant cause of the intensification of CS in the high latitude area and the decrease of CS in parts of the tropics, while in areas where SM is drier, STMP may weaken the former's negative effect on CS. Besides, simulation results based on medium emission scenarios indicating that CS may increase by about 36% by the end of this century. These results highlight that a more comprehensive understanding of the magnitude and driving mechanism of the soil minerals' CS is the key to realizing their potential as a nature-based climate solution.

**Key words:** Chemical weathering; Carbon sink; Soil minerals; Climate change; carbon budget

## Introduction

There is still a carbon imbalance of about 0.1-0.6 Pg C $yr^{-1}$ in the current carbon cycle system(Stocker et al., 2013, Fig. 1), previous studies have regarded the carbon sink (CS) produced by chemical weathering of rocks as the key to solving the carbon imbalance problem, and have estimated the magnitude and pattern of the CS of various rocks based on this (Hartmann, 2009; Li et al., 2018; Romero-Mujalli et al., 2018; Xi et al., 2021). However, due to the shielding effect of the soil layer, the chemical weathering flux budget of the underlying bedrocks often loses more than 40% under natural conditions (Hartmann et al., 2014), and the main reason is the incomplete weathering of rocks, resulting in the formation of smaller primary and secondary minerals distributed in the soil, such as feldspar, pyroxene, chlorite, smectite and mica, etc (Zolkos et al., 2018). These minerals can not only store about 600Pg of organic carbon per year (Ferdush and Paul, 2021), but also absorbing a certain scale of inorganic carbon through chemical reaction with $CO_2$ in the atmosphere/soil (Doetterl et al., 2018), especially for most clay minerals with silicate as the main component, they are not only widely distributed, but also having a large specific surface area for reaction, resulting in a high degree of stability of the carbon sink effect on the geological time scale (Bibi et al., 2016; Whitfield et al., 2018). Therefore, estimating the magnitude and pattern of the weathering CS of clay minerals can not only provide new ideas for solving the problem of carbon budget imbalance, but also will hopefully update the understanding of soil carbon pools.

The weathering of minerals in the soil can not only generate CS, but also can release lots of basic cations, which play a key role in maintaining the development of terrestrial ecosystems and mitigating the harm of acid deposition. Therefore, scholars have done a lot of modeling and inversion for the chemical reaction kinetics of various minerals in the soil (Goddéris et al., 2006; Olsson et al., 1993; Sverdrup and Warfvinge, 1993; Sverdrup and Belyazid, 2014), and then estimated the ability of the minerals to release cations (that is, the weathering rate of the soil). For example, Erlandsson et al estimated the soil weathering rate at the site scale based on long-term measured results and the PROFILE model (Erlandsson et al., 2016), similarly, Roy et al used the same model and the ISRIC-Wise database to estimate the ratio of basic cation to Al concentration on a global pixel scale (Roy et al., 2012). At the watershed scale, Goddéris et al (2006) considered the migration of chemical elements between different layers of soil, and using the WITCH model to estimate the weathering rate of the soil on the granite bedrock, on this basis, Roelandt et al (2010) and Beaulieu et al (2011) estimated the distribution characteristics of weathering rate and CS in pixels based on the spatial distribution map of minerals in the soil, respectively. Therefore, it can be seen from previous studies that based on a suitable kinetic model and soil mineral distribution map, it is expected to estimate the spatial distribution pattern of CS produced by chemical weathering of minerals in the soil. It can be seen from previous studies that based on a suitable kinetic model and the soil minerals distribution map, it is expected to estimate the spatial distribution pattern of CS of soil minerals. However, due to the lack of data on the spatial distribution of soil physical properties and mineral composition at the global scale, only a few studies have discussed the CS of minerals weathering in soil at the site and small watershed scales (Beaulieu et al., 2011; Goddéris et al., 2013), studies on the magnitude and temporal and spatial distribution of weathering CS of soil minerals, especially clay minerals, have not yet been discussed on the global pixel scale.

In addition, the weathering of minerals in the soil is very sensitive to the disturbance of climate change. For example, the experimental results of Akselsson et al (2016) in Sweden showed that warming temperature can increase the weathering rate of minerals in the soil by more than 20%, and the study by Yu et al (2020) in the subtropical regions of China found that regional warming reduced the basal cation concentration of soil weathering. Previous studies have shown that soil water is also an important factor affecting soil weathering (Kronnäs et al., 2019), but as soil moisture (SM) in most regions of the world decreases (Deng et al., 2020), Not only the chemical weathering process of rocks may be weakened (Xi et al., 2021), the weathering of soil minerals is also affected (Yu et al., 2020), especially in arid and semi-arid areas, SM is not only an important factor in controlling the soil carbon pool (Zhao et al., 2019), but the drought can cause a large amount of soil carbon pool loss, especially the bottom soil carbon pool (Canarini et al., 2017; Soong et al., 2021; Su et al., 2020). Therefore, in the context of global warming and soil drying (Deng et al., 2020), evaluating their respective effects on CS of soil minerals is of great significance for correcting soil weathering models and re-understanding soil inorganic carbon pools.

Hence, based on the widely used steady-state soil geochemical profile model (PROFILE model), and using the newly released spatial distribution map of the global clay mineral content (Ito and Wagai, 2017), we estimated the monthly-scale CS of clay-grade minerals in the global soil from 1970 to 2018, aiming to discuss the following questions: 1) What is the magnitude, pattern and evolution trend of the CS of the chemical weathering of clay minerals in the soil? 2) What are the spatial characteristics of the effects of global warming and soil drying on CS of soil minerals? 3) How does the CS of soil minerals compare with other CS?

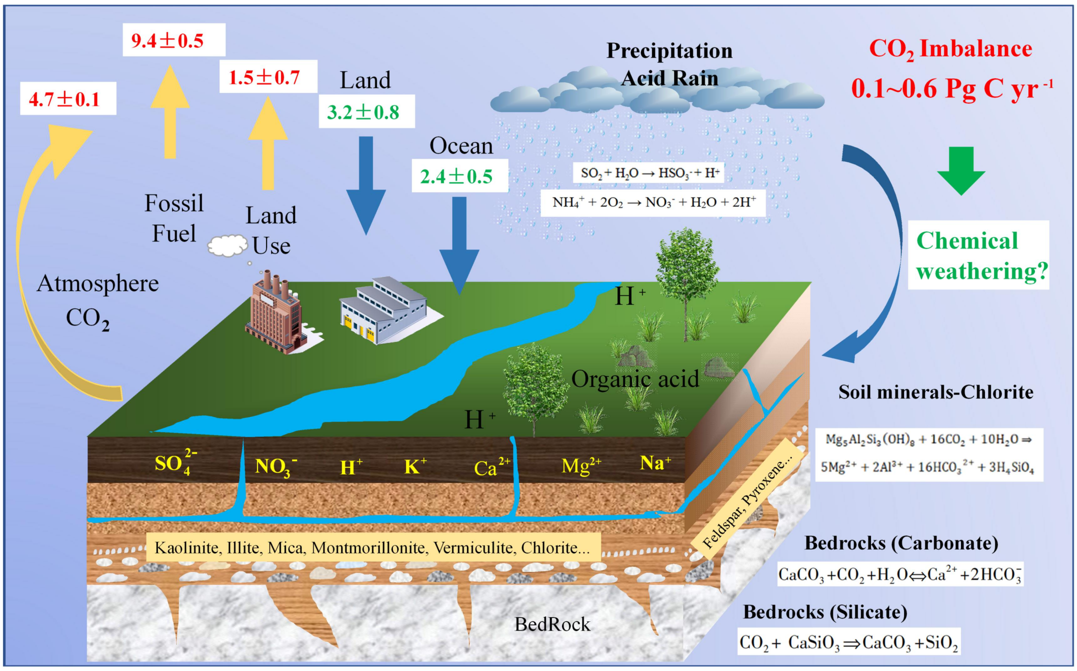


Fig. 1 Schematic diagram of the global carbon budget from 2008 to 2019

## Results

### *Spatial differentiation of carbon sink*

In terms of magnitude, combined with the chemical formula of typical mineral weathering (Goddéris et al., 2006), we have summarized the CS of clay minerals in soils at depths of 0-200 cm around the world. It was also found that the annual average carbon sink flux (CSF) of five types of clay minerals (including chlorite, smectite, illite, mica, and vermiculite) was about 0.50 t C $km^{-2}$, and the total CS was about 110.86 Tg C $yr^{-1}$, which accounts for about 34% to 42% of the CS of rocks (Hartmann., 2009) and about 18% of the missing carbon sink (Xi et al., 2021), in addition, the magnitude of this CS is basically equivalent to the CS of global silicates (Zhang et al., 2021). Based on the statistics of climate zones, it is found that the CSF (2.43 t C $km^{-2}$) and carbon storage (59.69 Tg C $yr^{-1}$) in tropical are much higher than other climate regions, followed by temperate (20.83 Tg C $yr^{-1}$), arid (18.17 Tg C $yr^{-1}$), cold zone (11.60 Tg C $yr^{-1}$) and polar zone(0.58 Tg C $yr^{-1}$) (Table S1). In addition, affected by the mineral content, the capacity of CS clay minerals in the soil is positively correlated with soil depth, the average CS at depths of 0-10cm, 10-40cm, 40-100cm, and 100-200cm are about 6.77 Tg C, 21.22 Tg C, 33.10 Tg C, 49.77 Tg C, etc. (Fig. 3), the CSF increases with depth, and the average values of CSF are 0.03 t C $km^{-2}$, 0.10 t C $km^{-2}$, 0.15 t C $km^{-2}$, and 0.23 t C $km^{-2}$, respectively.

In terms of spatial distribution, the high-value areas of CSF are mainly concentrated in the range of 30° north-south latitude, and the low-value areas are mainly distributed in areas above 30°N in the northern hemisphere, such as Russia, Canada, and Alaska. Affected by soil thickness, there are differences in CS at different depths in the same area. For example, in the karst area of southwest China, despite abundant hydrothermal conditions, most of the soil thickness in this area is less than 1 meter (Li et al., 2020), so the high value of CSF is mostly only within the depth of 0 to 100cm, while the CS potential of minerals at the depth of 100-200cm is greatly reduced (Fig. 2d). However, in the Amazon River Basin in South America, due to the large runoff and serious surface soil erosion (Flores et al., 2019), the mineral content in the soil is low, so the CSF of the minerals in the surface soil is also very low (Fig. 2a), but the CS of soil below 40cm starts to increase (Fig. 2c). In addition, near the Congo Basin in Africa, high temperature and drought have reduced the water content of the topsoil (Zhu et al., 2021), which will also limit the CS of potential of the topsoil, while in the subsoil, with the increase of soil moisture Increase, this restriction has been alleviated.

At different latitudes, the CSF presents an obvious three-peak distribution. Taking the latitude profile of CSF at a depth of 0 to 200 cm as an example (Fig. 2e), the CSF of world's major clay minerals first increase and then decrease from north to south, among them, the average CSF in the 30°N-60°N latitude zone is mostly lower than 1 t C $km^{-2}$. From 30°N to the south, the CSF gradually increases, in the range of

17°N to 24°N, the average CSF is higher than 2.0 t C km$^{-2}$, and in this latitude zone, the CS of it accounts for about 7.4% of the global. Moreover, the CSF reached its first peak (2.80 t C km$^{-2}$) near 18°N. Thereafter, to the south, the CSF first decreased and then increased, and reached the second peak (3.47 t C km$^{-2}$) near 8°N. The average CSF in the range of 7°N to 11°N is higher than 3 t C km$^{-2}$, and the CS in this latitude zone accounts for a higher proportion (9.7%). The third peak appeared near 3°S (3.31 t C km$^{-2}$), and the average CSF in the latitude zone between 0°S and 5°S reached 2.75 t C km$^{-2}$, and the CS accounted for about 10.64%.

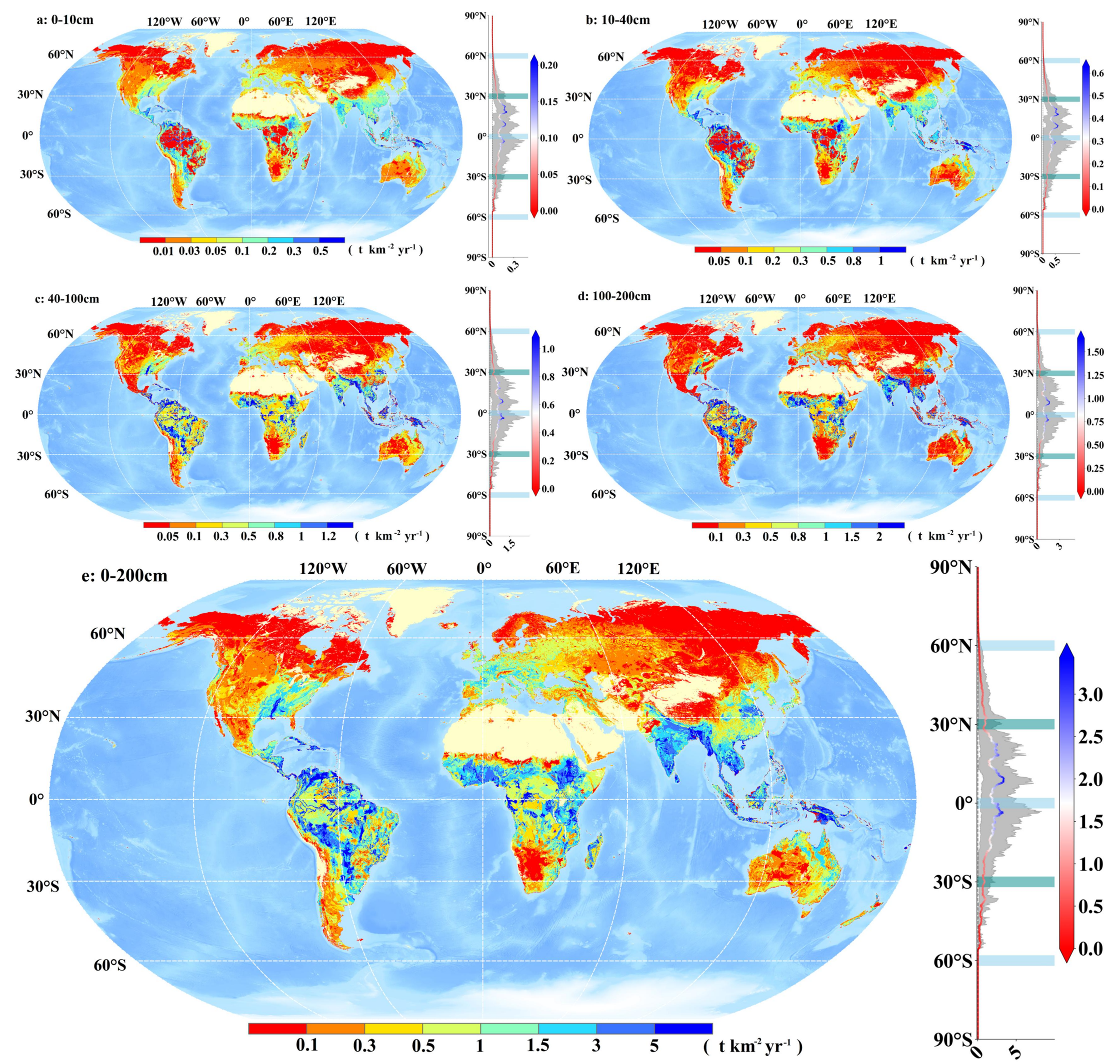


Fig. 2 Spatial and latitude distribution map of global weathering carbon sink of major clay minerals

### ***Spatial differentiation of carbon sink trends***

Clarifying the temporal and spatial evolution characteristics of CS of soil minerals is of great significance for understanding the fluctuations of regional or global soil inorganic carbon storage. To this end, we analyzed the magnitude and spatial evolution trends of CS of five major types of clay minerals in the world from 1970 to 2018. The results show that the change trend of CS of clay minerals at different depths basically shows a fluctuating upward trend, and the change trend is significant (Fig. 3). The growth rate increases with soil depth, from 0.007 Tg C $yr^{-1}$ to 0.1 Tg C $yr^{-1}$ in 0 to 200 cm deep soil, and the average growth rate of global CS is 0.17 Tg C $yr^{-1}$. This rate is higher than the change trend of CS of major rocks in recent years (0.1 Tg C $yr^{-1}$), but lower than that of carbonate rocks (0.31 Tg C $yr^{-1}$) (Xi et al., 2021).

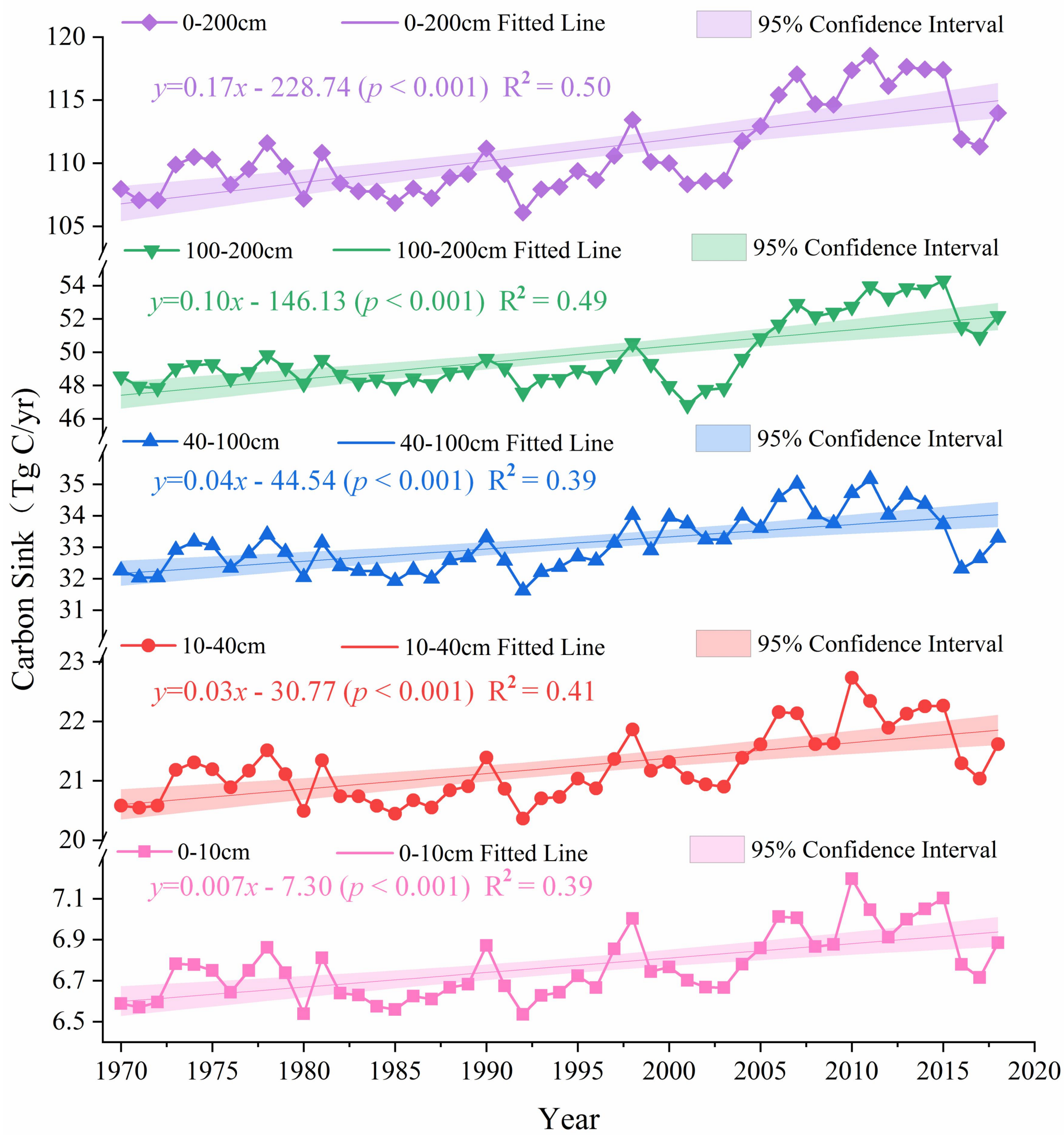


Fig. 3 Change trend of carbon sink of clay minerals at a depth of 0 to 2m from 1970 to 2018

Spatially, we estimated the changing trend of CS in soil at different depths on a pixel scale (Fig. 4), and founding that the trend of CS in clay minerals is opposite to that of silicate rocks (-0.027 t C $km^{-2}$ $yr^{-1}$) (Zhang et al., 2021), in the 0-200cm depth of soil, the CS of clay minerals in about 56.47% of the world has shown a significant increase. Since 1970-2018, about 1.4 kg of more carbon can be sequestered per kilometer per year on average. In addition, the growth rate of CS in the bottom soil (100-200cm) is about 8 times that of the surface soil (0-40cm), which indicating that the carbon storage of minerals in the bottom soil has been increasing in the past half century, and the role of balancing the carbon cycle of the minerals in the bottom soil is growing. Most of the CS in the northern hemisphere above 30°N are growth-oriented, and the high-value areas of growth are mainly concentrated in the Indian Peninsula, the Nile River Basin, the Amazon River Plain, South America near the Caribbean, and the middle and lower reaches of the Yangtze River in China.

Combined with the climate zoning map, we found that in tropical regions, the significant increase or decrease of surface soil (0-40cm) is basically the same, and the rate of CS is negative, indicating that the carbon sequestration capacity of surface soil in tropical regions is weakening. However, the growth rate of CS in the bottom soil can offset the deceleration of CS in the surface soil, eventually, the CS in the tropics are still mainly increasing. In addition, although the CS in the temperate zone is higher than that in the arid zone, the growth rate of the CS in this region is smaller, which indicating that the potential CS of minerals in the soil is gradually increasing in the arid zone. In the cold and polar zone, the CS of 71.89% and 55.17% of the regions are increasing significantly, respectively.

In the latitude zone, the overall trend of CS increasing firstly and then decreasing from north to south. Taking the profile of the CS trend at a depth of 0-200 cm as an example (Fig. 4e), in the range of 20°N to 60°N, the trend of CS is mostly positive. In the range of 5°N to 15°N, the rate of CS is mostly greater than 4.5 kg C $km^{-2}$ $yr^{-1}$, and a peak value (8.05 kg C $km^{-2}$ $yr^{-1}$) appears near 14°N, and then, the change trend of CS turned negative as the latitude decreased, and the lowest value (-3.57 kg C $km^{-2}$ $yr^{-1}$) appeared near 11°S. The decreasing trend in the southern hemisphere did not gradually turn positive until around 35°S, and reached a peak again around 52°S (8.65 kg C $km^{-2}$ $yr^{-1}$).

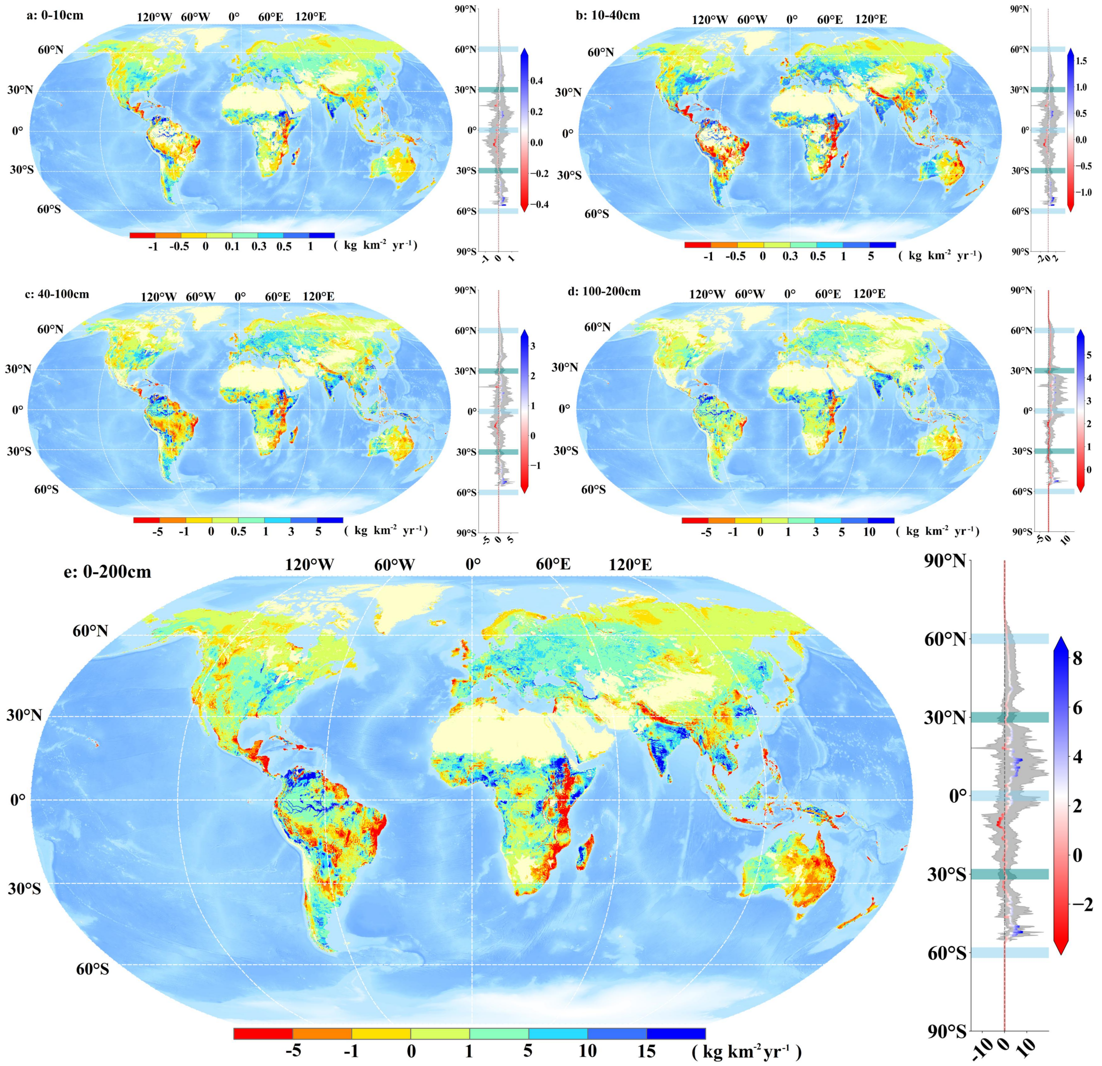


Fig. 4 Spatial and latitude differentiation of the change trend of clay mineral weathering carbon sink

***The influence of soil moisture on carbon sink of clay minerals***

Evaluating the impact of changes in soil hydrothermal properties on the CS of clay minerals at different soil depths is of great significance for understanding and improving the response mechanism of soil inorganic carbon storage to climate change. Based on the method mentioned in 2.2.3, we separated the relative contribution of SM and STMP to the CS of clay mineral weathering. The relative contribution of SM at a depth of 0-200cm is shown in Fig. 5. Although the area of the positive contribution area (52.91%) is slightly larger than the negative contribution area (47.08%), the average pixel value is -2.4%, which indicating that the SM has a negative effect on the weathering of clay minerals as a whole.

Spatially, the area where soil moisture is negatively affected are mainly concentrated in the southern hemisphere. Except for Western Australia, Western Africa, and Western South America, the influence of SM in other areas is mostly negative, while in areas above 30°N north latitude, the area where the soil moisture has a positive contribution is larger. In terms of latitude, the negative influence area of SM is mainly concentrated in the latitude zone of 30°N to 25°S. The highest value of the relative contribution of SM appears near 70°N (29%), and the lowest value appears near 12°S (-34%).

In climatic zones, the contribution of SM varies greatly in space. In tropical and temperate zones, the SM is mostly shows a negative contribution, especially in the soil with a depth of 0 to 100cm, the negative contribution of SM in the tropics is the highest (-24.28%). In the arid zone, the contribution of surface soil moisture is negative, but as the soil depth increases, the contribution of SM becomes positive, which further illustrating the potential of CS of minerals in the deep soil of the arid zone. In cold and polar zones, SM has a positive contribution, which may be related to the moistening of the soil in the high latitudes of the northern hemisphere in recent years (Deng et al., 2020).

Combining with the change trend of soil moisture (Fig. S1), we found that in the 0 to 100cm depth of soil, the average relative contribution of the area with reduced SM is -23.59%, and the average contribution of about 78.4% of the regional soil moisture is negative. The average contribution of 78.4% of the SM in this area is negative, which indicating that the surface soil moisture does weaken the weathering CS of clay minerals when there is a drying trend. However, in the bottom soil, this weakening effect is somewhat reduced, with a relative contribution of about -11.48%

at a depth of 100-200cm, and an average of about 88.72% of the area shows a negative contribution area.

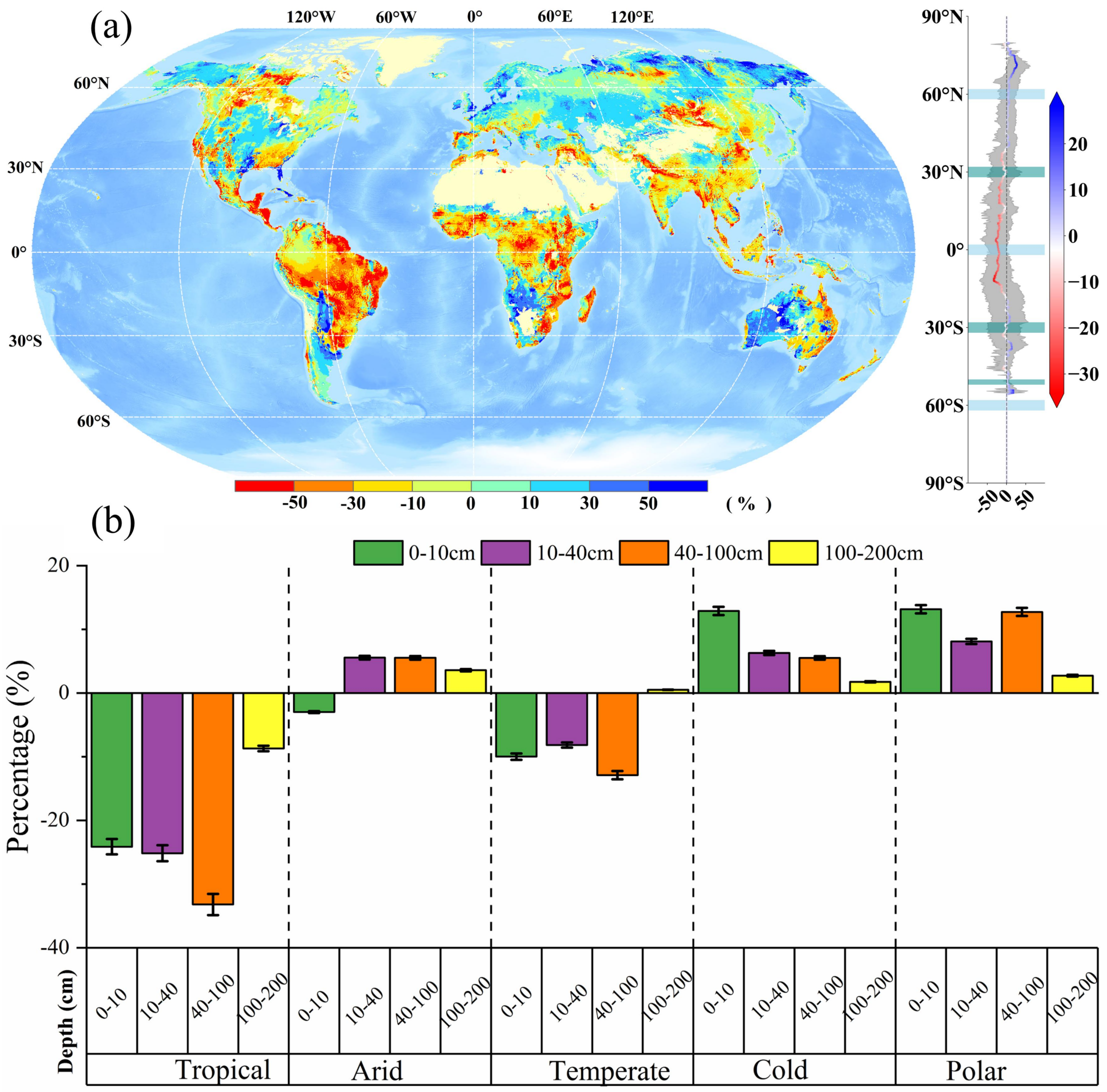


Fig. 5 Spatial differentiation of the relative contribution of soil moisture

***The influence of soil temperature on carbon sink of clay minerals***

The relative influence of STMP is shown in the figure below (Fig. 6). The results show that in the 0-200cm deep soil, the average value of the STMP is 3.29%, and more than half of the area shows a positive contribution (55.90%) ), which indicating that STMP accelerates the chemical weathering of minerals in soil, which is consistent with previous research conclusions (Akselsson et al., 2016).

In terms of spatial distribution, areas where STMP shows a negative contribution are mostly consistent with SM, but the contribution of STMP is less than that of SM. The positive contribution of the high value of STMP is mainly concentrated in the middle and high latitudes of the northern hemisphere, and the overall characteristics are similar to the relative contribution of SM. In terms of latitude differentiation, the overall characteristics of STMP are less significant than that of SM. The average contribution of STMP in most latitude zones is around 0, while the average value in areas above 60°N is mostly shows positive. However, the variability in areas above 75°N is extremely large, which may be disturbed by the data itself, but the CSF in these areas is low, so it has little impact on the overall situation.

In climatic zones, the contribution of STMP is quite different (Fig. 6b). It can be seen that the contribution of STMP in tropical and temperate zones is all negative, while the contribution in the arid, cold and polar zones are basically positive, and the average contribution in the arid zone is the highest (8.23%), which indicating that in arid regions, SM and STMP both promote the carbon sequestration of soil minerals. Combining with the spatial map of the change trend of STMP (Fig. S2), we further found that in areas where STMP is rising, the average relative contribution of STMP is 10.51% (0-40cm), and there are about 70.55% of the area showed a positive contribution on the whole. Although the average relative contribution in mid to deep soil is only 0.5% (40-200cm), in areas where the soil is warmed in the middle and deep layers, there is still 61% of the area where the contribution of STMP is positive. It further shows that when the STMP is warming, it does promote the CS of clay minerals, and this effect mainly occurs in the surface soil.

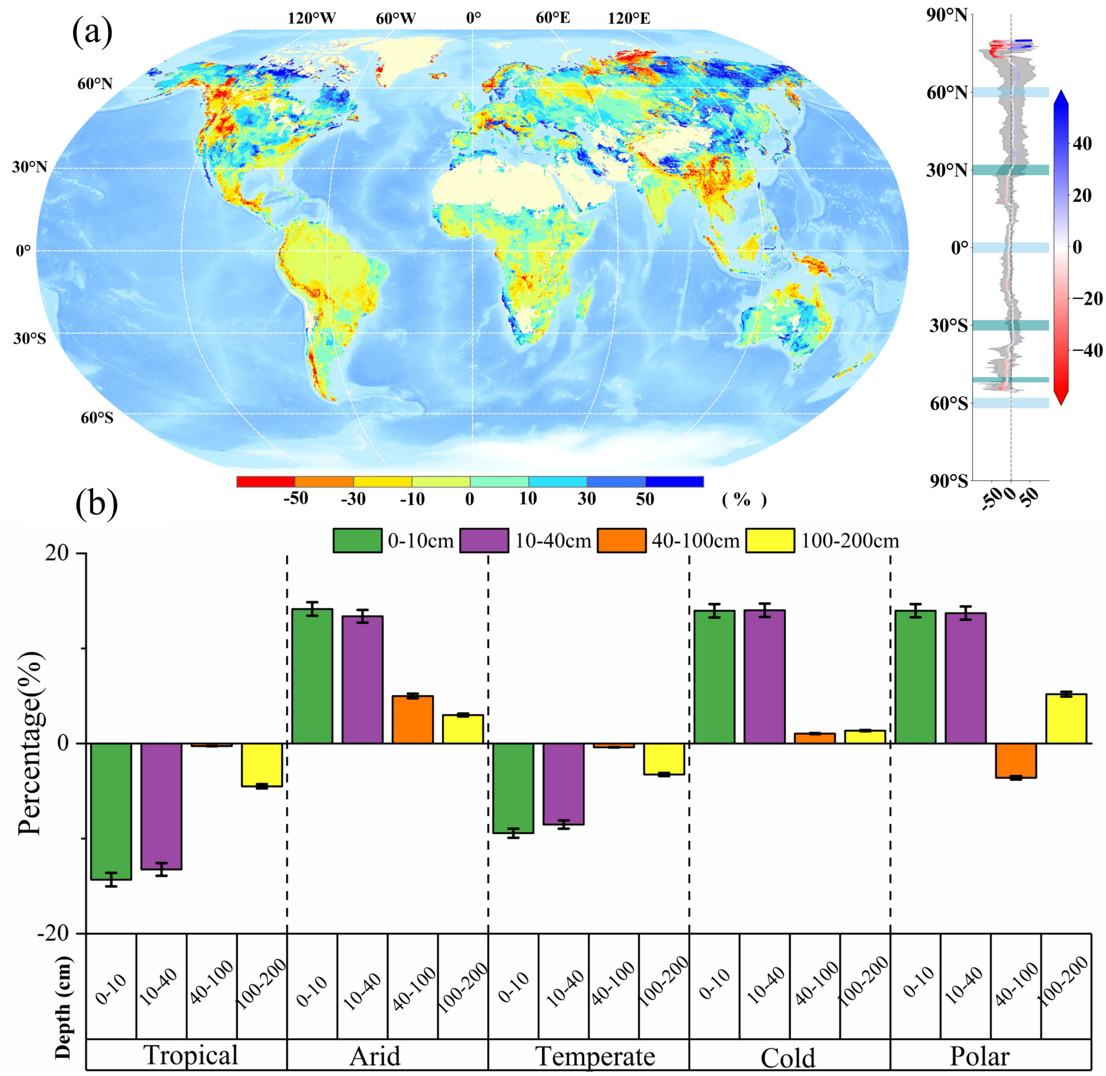


Fig. 6 Spatial differentiation of the relative contribution of soil temperature

## Discussion

### *Evaluation of our results*

In order to verify our estimated results, we carried out comparisons and discussions from site monitoring results, simulation results of other models, and research results of other scholars, respectively. Since there is no research on the global CS of clay mineral weathering, we first compared the soil weathering cation site data published in the National Nitrogen and Sulfur Deposition Database (Fig. 7a). This data set consists of the estimation results of multiple models and a summary of the measured data. The average value of cationic weathering at these sites is 1046.23 eq

$ha^{-1}$, and our result is 174.92 eq $ha^{-1}$, with an average proportion of 20.65% and a median of 9.70% (Fig. 7b), and it can be seen that the ratio is lower in the western United States, while higher in the eastern United States, which may be caused by higher soil temperature and soil moisture in the eastern United States than in the western United States. In general, the results of this paper are lower than the data of the site, but since only five types of minerals are considered, and the more easily weathered feldspar, pyroxene and other minerals are not considered, the estimated result is definitely lower than the overall weathering rate. However, because the values are in the same magnitude, the results have a certain degree of reliability as a whole.

In order to further verify the reliability of the model and the results, we compared the calculation results of two different models. First, we estimated the weathering rate of chlorite, mica and vermiculite with reference to a simple mineral model (Sverdrup and Warfvinge, 2018) with some site data in the ISRIC database (Fig. 7c), it turns out that our result is slightly smaller than the estimation result of the simple mineral model, and the average is about 0.8 times that of the latter, but most of the sample points are at the same magnitude. This further implies that our estimation results are more reliable.

In addition, we also used another set of more general model to characterize soil weathering in watersheds which named WITCH (Goddéris et al., 2006). This model assumes that each layer of soil is an independent box shape, and the weathering module of it also considering the weathering kinetics of silicate minerals, and this model can be used to simulate the soil weathering rate at the pixel scale in a small watershed (Roelandt et al., 2010). Therefore, we used this model to estimate the CS of smectite and illite (Fig. 7d, e). The results show that the CSF of smectite estimated using the WITCH model is smaller than that of the PROFILE model, but the CSF of illite is higher than the latter. Due to the complexity of soil minerals, the parameter settings between different models are quite different. Previous studies have also found that the estimation results between different models can differ by several orders of magnitude (Erlandsson et al., 2016), but our research show that the results between different models are almost on an order of magnitude, which once again shows that our results are highly reliable.

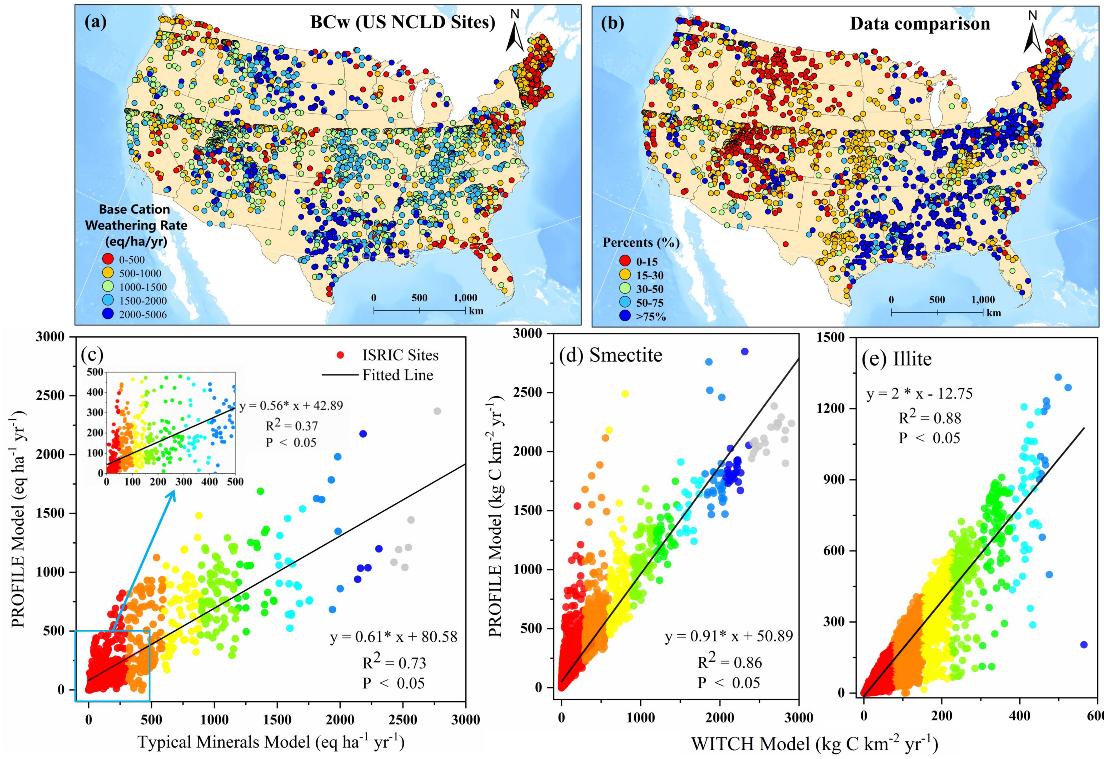


Fig. 7 Comparison of results. The Fig. 7a shows the distribution of the US nitrogen and sulfur deposition database, the Fig. 7b shows the ratio of the estimated results to the site data, the Fi. 7c shows the comparison of the weathering rate estimated by the PROFILE model and the typical mineral model, and the Fi. 7d and Fi. 7e show the comparison of the carbon sink flux estimated by the PROFILE model and the WITCH model.

In addition, we have also compared the research results of other scholars (Table 1). In terms of CS, our results are basically consistent with the deduction results of other studies, and are equivalent to CS of silicate, but smaller than the CS of rocks. In terms of CSF, we compared with the CS results of mineral weathering in loess and founding that our results are within its range, however, since carbonate minerals that are more susceptible to weathering were not considered, the value was low. In addition, although the CS is equivalent to that of silicate rocks, due to the limited distribution of silicate rocks, its CSF is higher than our results. In terms of weathering rate, we compared the weathering rate on site and regional scales. Although the weathering rate is lower than the results of other studies, the ratio is in the range of 13% to 32%. Therefore, this result is more consistent with the comparison result of the US National Nitrogen and Sulfur Deposition Database.

Table1 Comparison with other research

| Compared Target | Object | Region | This Study | Others’ | References |
|---|---|---|---|---|---|
| Carbon Sink (Pg C) | Soil | Global | 0.11 | 0.12 | Andrews and Schlesinger, 2001 |
| | Silicate | | | 0.13 | Zhang et al., 2021 |
| | Rocks | | | 0.32 | Xi et al., 2021 |
| Carbon Sink Flux ($t\ C/km^2$) | Loess | America | 0.7 | 0.6~2.4 | Goddéris et al., 2013 |
| | Silicate | Global | 0.5 | 1.67 | Zhang et al., 2021 |
| Weathering Rate (Eq/ha) | Forest Soil | Sweden | 44 | 224~332 | Akselsson et al., 2016 |
| | | Västra Torup | 169 | 530~575 | Kronnäs et al., 2019 |
| | | Hissmossa | 47 | 152~180 | |

***Synergistic and Trade-off effects of SM and STMP on CS***

Under natural conditions, soil moisture and soil temperature do not individually affect the weathering of minerals, and they interact to promote or limit the weathering process of minerals. For this reason, we further discussed the synergistic and offset effects of SM and STMP on the CS of clay mineral weathering. By superimposing the distribution map of the relative contribution of SM and STMP, we found (Fig. 8) that the land area driven by the two together accounted for about 43.17% of the total land area. It can be seen that the area of the main control area of STMP is higher than that of SM (Fig. 8b). Among them, the areas where both soil moisture and soil temperature contribute positively accounted for about 28.7%, with an average relative contribution of 44.9%. They are mainly distributed in the northern hemisphere, especially in high latitudes. This phenomenon is consistent with the results of other scholars (Zolkos et al., 2018), which may be related to the significant warming in the high latitudes of the northern hemisphere in recent years. The melting of frozen soil in high latitudes not only exposes minerals, but also makes the soil environment warm and humid, which is very conducive to weathering reactions (Cuozzoa et al., 2020).

The area where SM and STMP are both negatively contributing account for about 14.47%, and the average contribution on the pixel is -51.04%. That is to say, both SM and STMP have led to a reduction of more than half of the CS of clay minerals in this area, which is mainly distributed in most parts of the southern hemisphere, especially in climatic regions such as tropical and temperate zones, the reason may be that the soil moisture in these areas is greatly reduced (Deng et al., 2020).

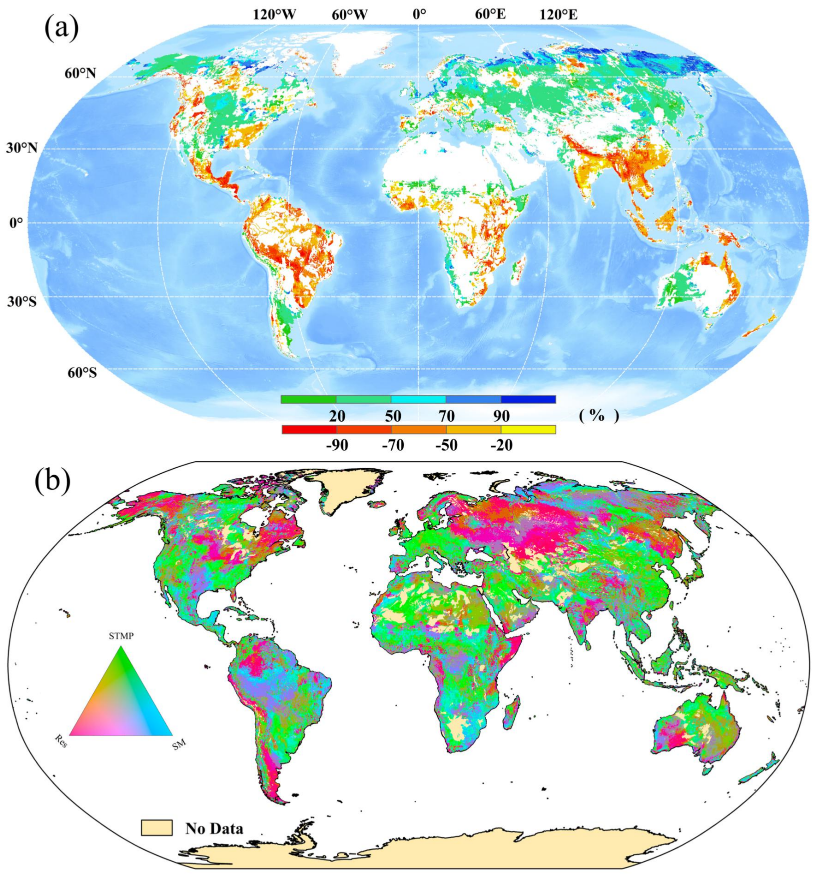


Fig. 8 The synergistic effect of soil moisture and soil temperature. Fig. 8a is the area where soil moisture and soil temperature are both promoted or weakened, and Fig. 8b is the main control area of different factors

Combined with the change trend of SM, we further found that in areas where SM dries out and SM is negatively affected, the average relative contribution of STMP is 1.60%, and in 55.06% of this area, the influence of STMP is positive (Fig. 9a, b), indicating that in more than half of the area, STMP may offset part of the negative impact of soil moisture drying on the CS of clay minerals.

However, combined with the change trend of soil temperature, we found that in areas where soil warming and the contribution of STMP is positive, the average relative contribution of SM is 20.21%, and these areas are mainly concentrated in the high latitudes of the northern hemisphere (Fig. 9c, d), the reason further validates the findings in the previous section that warming can lead to soil warming and soil wetness in high latitudes, which to some extent accelerates the chemical weathering process of minerals in the soil.

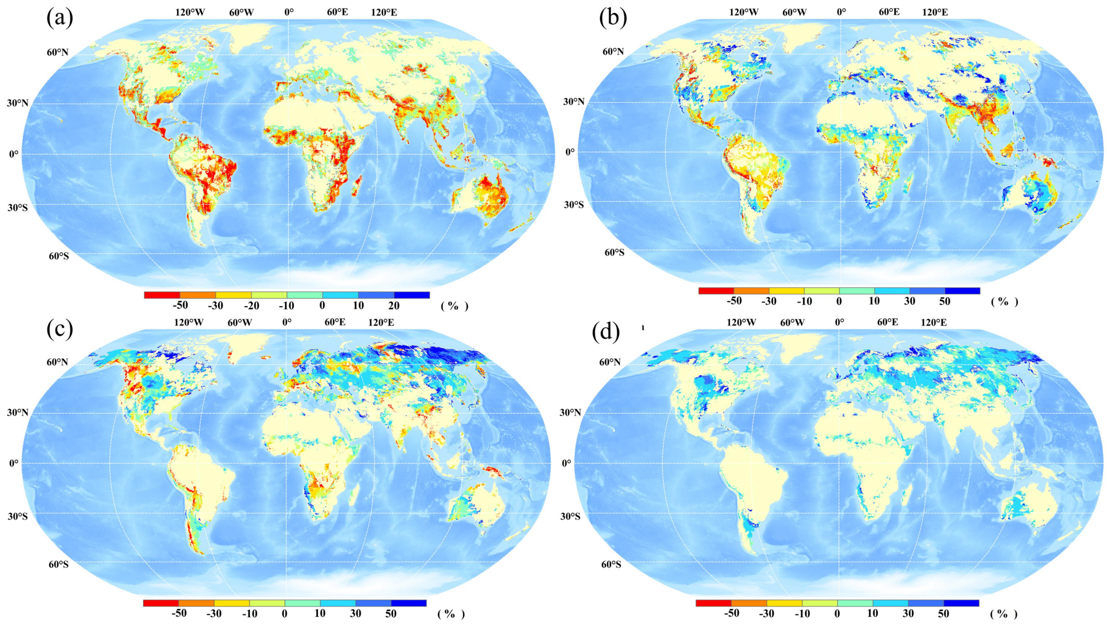


Fig. 9 The offset effect of soil moisture and soil temperature. The Fig. 9a shows the relative contribution of soil moisture in the soil desiccation area, the Fig. 9b shows the relative contribution of soil temperature in areas where the soil is drying and soil moisture is showing a negative contribution, the Fig. 9c shows the relative contribution of soil temperature in the soil warming area, the Fig.9d shows the relative contribution of soil moisture when the soil is warming up and the soil temperature is positively contributing to the area.

***Trends of CS in future scenarios***

Referring to the SM and STMP data based on the medium emission scenario RCP4.5, we used the PROFILE model to extend the global CS of clay minerals from 2051 to 2100 (Fig. 10). Under the RCP4.5 scenario, the average weathering CS of the world's major clay minerals is about 0.15 Pg C $yr^{-1}$, which means that after government intervention, the high concentration of carbon dioxide emitted in the future can still increase the capacity of CS in clay minerals by about 36%. In general, CS of clay minerals shows a trend of rapid increase first, and then a slow decrease, however, there are slightly differences in different climate zones. For example, in tropical with the largest amount of CS, the trend is basically a continuous increase, but in temperate areas, CS shows a trend of first increasing and then decreasing.

In addition, combined with the future trends of SM and STM, we extracted the percentage changes of CS in drier and warmer soil regions. The results show that the trend of CS in these regions is basically the same as that of CS that have not been partitioned, which shows that under the future medium emission scenario, the CS will be affected by soil desiccation and soil warming slightly less than the current impact. The reason for this phenomenon may be related to the high concentration of carbon dioxide emitted. For example, in the study of Roelandt et al (2005), it was found that high concentration of $CO_2$ can increase the cations released by minerals after weathering by about 20%. Furthermore, the positive impact of soil warming on weathering may also offset the negative impact caused by the reduction of SM, for example, based on future climate simulation experiments, Akselsson found that by 2050 the temperature rising can increase the weathering rates of soil minerals by up to 30% (2016).

High-concentration carbon emissions not only mean an increase in climate warming, but also accelerating the growth rate of vegetation (Chen et al., 2021), which in turn will indirectly participating in the weathering reaction of minerals by affecting the hydrological environment of soil. The changes in these environmental factors in the future will have a certain degree of impact on the weathering process of minerals. However, due to the limitation of data resolution, we did not conduct a detailed analysis and only estimating the change trend of CS in clay minerals in the future, and the above results suffice to illustrate the potential of clay minerals in the soil as a stable carbon-sequestrated method in the context of possible intensified climate warming in the future.

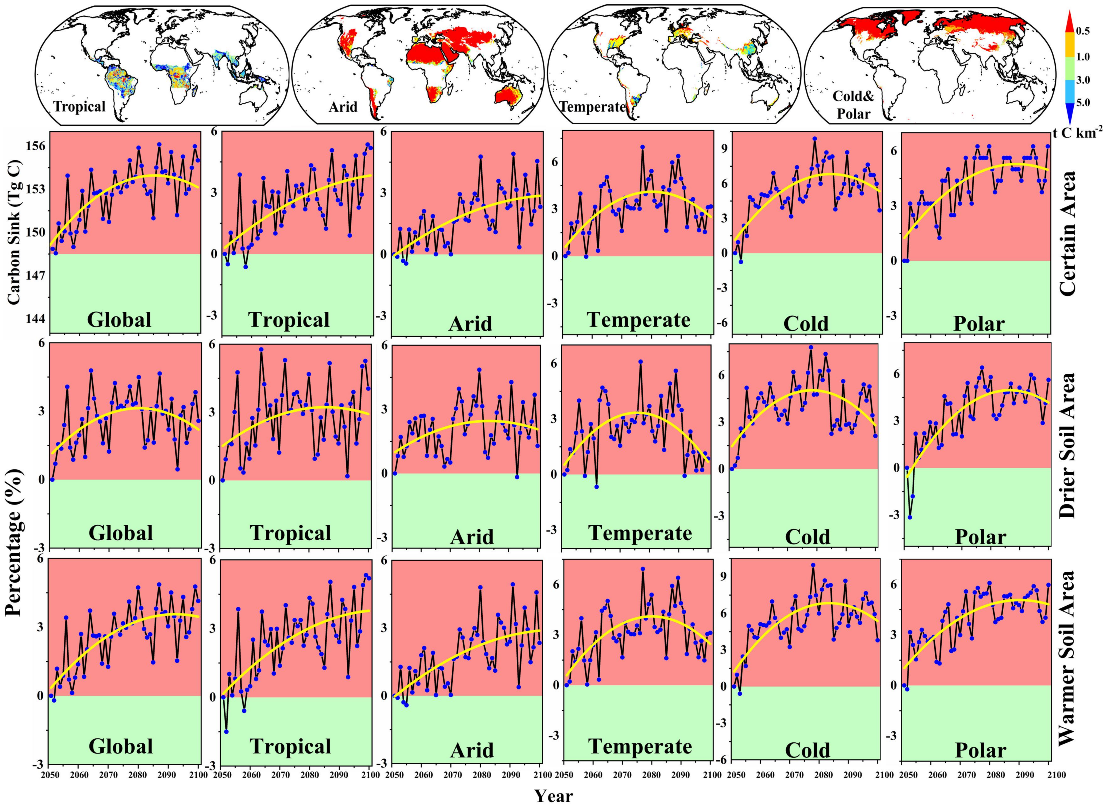


Fig. 10 Time series of CS and its trends under the medium emissions scenario RCP4.5 in the different areas. The top four maps represent the distribution of global clay minerals' carbon sink flux in different climatic regions. The line chart shows the changing trends of carbon sink in the world and in different climatic regions. Among them, except that the unit of the ordinate of the first line chart is carbon sink, the rest are expressed as the percentage of changes in carbon sink in other years compared with the carbon sink in 2050.

***The uncertainty of this study***

Given that the chemical formula of the mineral itself is extremely complex, our study only refers to the typical chemical formula of the mineral determined in the laboratory by the predecessors (Goddéris et al., 2006). However, the actual situation is very complicated and the weathering evolution stage between different minerals is not considered, for example, the mica may be weathered first to form illite and then subjected to secondary weathering. So our thinking is consistent with estimating the CS response of the weathering of the bedrock, that is, the estimated CS after the minerals are completely reacted (Hartmann et al., 2009). Therefore, the results estimated in this paper are theoretically potential CS.

Although the content distribution map of clay-grade minerals has been widely cited (Ito and Wagai, 2017), under natural conditions, this set of data still has certain uncertainties. By summarizing the uncertainty of the mineral content on the surface and bottom grids, we know that the average value on the pixel is about 36.52%. Therefore, the estimated CS based on this data set should also have a considerable degree of uncertainty.

The PROFILE model itself has a high degree of uncertainty. Even under the premise of ensuring the quality of the input data, the error of the model can reach about 40% (Jönsson et al., 1999), when compared with the soil weathering results of other models, the error can reach 33%~300% (Futter et al., 2012), which is mainly affected by the input data. Although some remote sensing and hydrological data are used in this paper, there are still uncertainties. For example, the error of evapotranspiration data in the land surface model assimilation data product (GLDAS) in East Asia can be as high as 40% (Khan et al. , 2018), and the SM is lower than the observed value (Deng et al., 2020). In addition, due to the low resolution of some data, downscaling methods such as resampling have to be used, and it is found that the average error in our data preprocessing process is about 6.22% through calculations,, and these errors are all errors generated in the data production process.

In addition, we only estimated the relative contribution of soil moisture and soil temperature, but we know from Fig. 8b that the main controlling factors in most areas have not yet been determined. Factors such as vegetation, $CO_2$ concentration, acid deposition, human activities and other factors will affect the process of soil weathering. For example, vegetation can control soil weathering by controlling soil hydrology, and the high $CO_2$ concentration of deep soil can increase the weathering rate by at least 15% (Roelandt et al., 2010), moreover, nitrogen deposition can cause global soil acidification and destroy the weathering reaction of carbonate minerals in the soil, causing the soil to release a large amount of $CO_2$ (L. Deng et al., 2020; Raza et al., 2020), therefore, all of the above factors will play a key role in the weathering of minerals in the soil.

In summary, due to the constraints of the original model, input data, influencing factors, etc., there are still a lot of uncertainties in our research results. However, after comparing with sites, other models, and other research results, we found that the results of CS in this paper have a certain degree of credibility. The greatest value of this paper is that we have produced a dataset of clay mierals in soil with high temporal and spatial resolution, and clarifying the contribution of the CS produced by the weathering of clay minerals to the carbon imbalance. These data and research results will provide more novel and unique ideas for re-understanding the soil inorganic carbon pool and improving the carbon cycle framework.

## Materials

### *Clay minerals*

This article refers to the latest global spatial distribution map of clay-grade minerals released by Ito and Wagai (2017), this data set compiles data including the content of the main clay minerals in the soil and their soil bulk density, etc.According to the classification of soil genesis, the percentages of minerals including kaolinite, smectite, vermiculite, chlorite, illite, mica and quartz were estimated, respectively. This data set is divided into two sets of surface and deep data, with spatial resolution ranging from 2'to 2°, and has been widely cited in the field of geochemical simulation (Charbonnier et al., 2020; Dabat et al., 2019).

### *Soil attribute dataset*

The soil moisture (SM), soil temperature (STMP) and other data used to simulate the CS of clay minerals come from the GLAS Noah 2.0 and GLAS Noah 2.1 data sets released by Global Land Data Assimilation System (LDAS-NASA) of NASA. Among them, the GLAS Noah 2.0 data set was used from 1970 to 1999, and the GLAS Noah 2.1 data set (https://ldas.gsfc.nasa.gov/gldas/) was used after 2000. This set of data is divided into 0-10cm, 10-40cm, 40-100cm, 100-200cm and other different soil layers according to the soil depth from top to bottom, with a spatial resolution of 0.25°, it mainly combines satellite and ground observation data, and uses advanced data assimilation and ground simulation technologies, which has been widely cited in the field of chemical weathering simulation research on rocks (Li et al., 2018; Gong et al., 2021) .

In addition, since the weathering reaction of clay minerals is limited by soil temperature, in frozen soil areas, too low temperature will inhibit the weathering process. Therefore, this paper estimates the percentage of frozen soil at the pixel scale from 1970 to 2018 based on soil temperature. The calculation formula is as follows:

$$r = \frac{\sum_{i=1}^{12} con(T_{soil} > 0,1,0)}{12} \tag{1}$$

Where, r is the annual percentage of frozen soil with %, and Tsoil is the soil temperature with K.

The soil bulk density data of the surface and bottom layers comes from the global clay mineral and its attribute database compiled by Ito and Wagai (2017). Compared with a single soil bulk density data, this data can finely describe the difference in soil bulk density between the surface and bottom soils. Among them, the average bulk density of the top soil is 1.32 $g/cm^3$, and the average bulk density of the bottom soil is 1.38 $g/cm^3$.

The soil covered by rock weathering often results in uneven soil thickness due to differences in lithology and local hydrothermal conditions. If the CS of global clay minerals is estimated at a thickness of 2m, the estimation result will inevitably be too high. To this end, this paper uses the absolute soil thickness data released by Oak Ridge National Laboratory (Pelletier et al., 2016) to correct the rate of mineral weathering in areas with different soil thicknesses.

***Climate attribute dataset***

As an important indicator of $CO_2$ concentration in soil, this paper uses evapotranspiration data to estimate the $CO_2$ partial pressure characteristics in the atmosphere/soil month by month (Li et al., 2019; Zeng et al., 2019). The formula is as follows (2):

$$\log(pCO_2) = -3.7 + 2.09 \times (1 - e^{-0.00172 \times ET}) \quad (2)$$

Here, ET is evapotranspiration with mm. The monthly scale evapotranspiration data from 2001 to 2014 comes from the MOD16/ET data set released by the University of Montana. Based on the 8-day resolution, monthly scale data with a global resolution of 0.05°×0.05° was produced. The evapotranspiration data for other years comes from the GLDAS Noah 2.0 and Noah 2.1 data sets provided by NASA.

In addition, in order to calculate the spatial differentiation of CS of clay minerals, we also used the latest Köppen climate classification map (Beck et al., 2018), this climate zoning data represents the current (1980-2016) climate background, with a spatial resolution ranging from 0.0083° to 0.5°.

***Site data***

This study refers to the soil weathering rate in the Critical Load Database of Nitrogen and Sulfur Deposition (NCLD) in the United States to compare with our estimated results of the weathering rate of clay-grade minerals, this database was developed by the United States Scientific Committee on Atmospheric Deposition Critical Load (Lynch, J.A et al., 2020), based on a set of databases shared by the United States Atmospheric Deposition Program (NADP). Among them, the key element used to evaluate the critical load is the weathering rate of minerals in the soil. In this database, a number of measured data including soil weathering rate, nitrogen and sulfur deposition are recorded in detail. The details of the site are shown in Figure 7a.

In order to verify our estimation results, we also used the WITCH model to recalculate, and used the site data in the ISRIC database (Batjes et al., 2020), this data set includes key parameters such as soil texture, soil temperature, and soil moisture on the site.

***Methods***

***POFILE Model***

We used the steady-state soil geochemical profile model (PROFILE) to estimate the weathering rate and CS of global clay minerals in soil. The PROFILE model is a steady-state mechanical soil biogeochemical model (Sverdrup and Warfvinge, 1993), it can be used not only to estimate the rate of soil weathering, but also to determine the critical load of acid deposition in soil and surface water (Erlandsson Lampa et al., 2020). This model couples independent reactions between minerals and different media, making it not only able to simulate the reaction process of minerals with a single medium, but also combining environmental data such as soil temperature and soil moisture, making the scale expansion is possible (Whitfield et al., 2018). In addition, the model also considers the influence of time on the weathering process, and can simulate the weathering rate under a long time sequence. The core formula is as follows:

$$R_{W}CO_2 = \sum_{i=1}^{minerals} R_i \times A_w \times x_i \times \phi \times Z \tag{3}$$

Where, $R_wCO_2$ is the total weathering rate of the chemical reaction of clay minerals in which carbonic acid participates, and Ri is the weathering reaction rate of the i-th type of clay minerals (Equations 4, 5), Aw is the reaction contact area of the mineral (Equation 6), $x_i$ is the content of the i-th clay mineral in the soil, $\phi$ is the soil moisture saturation (Equation 7), and Z is the soil thickness with m. The weathering kinetics module of the PROFILE model takes into account the reaction of soil minerals with water, $CO_2$, exogenous acid $H^+$ and organic acids. The formula for estimating the reaction rate of minerals with $CO_2$ at 8°C is as follows:

$$R_{i\text{-}8} = K_{CO_2} \times \left(\frac{P_{CO_2}}{1 + f_{CO_2} \times (P_{CO_2} + P_{CO_2 Limit})}\right)^{nCO_2} \tag{4}$$

Where, $R_{i\text{-}8}$ is the mineral reaction rate measured at 8° C in the laboratory, and $KCO_2$ is the mineral dissolution kinetic constant, and its value is often related to the temperature (Equation 8), $PCO_2$ is the partial pressure of carbon dioxide in the atmosphere/soil (Equation 2), $PCO_{2limit}$ is the limit of carbon dioxide absorption, $nCO_2$ is the reaction order, and $fCO_2$ is the suppression constant 1. After temperature correction, the following formula can be used to estimate the mineral reaction rate at room temperature:

$$R_i = e^{R_{i-8} \times A_w \times \left(\frac{1}{T_{lab}} - \frac{1}{T_{soil}}\right)} \tag{5}$$

Here, A is the Arrhenius index factor, with a fixed value of 3600K, $T_{lab}$ is the laboratory temperature of 8℃ (281.15 k), and $T_{soil}$ is the soil temperature in K. The mineral reaction contact area $A_w$ is mainly related to the content of clay, sand, and silt in the soil (Erlandsson et al., 2016). The estimation formula is as follows:

$$A_w = 8 \times X_{clay} + 2.2 \times X_{slit} + 0.3 \times X_{sand} \tag{6}$$

The moisture saturation $\phi$ in the soil is related to the soil water content, soil density, etc., and can be estimated in combination with the following formula:

$$\phi = \frac{\theta \times \rho_{soil}}{\rho_{soil} - \rho_i + \theta \times \rho_{water}} \tag{7}$$

Among them, θ is soil moisture, $\rho_{soil}$ is soil density, $\rho_{water}$ is water density, and $\rho_i$ is soil bulk density.

***Trend analysis***

We use time as the independent variable, and the year-by-year carbon sink flux at the pixel as the dependent variable, and combined the unary linear regression and F-test to estimate the change slope of the weathering CS of the world's major clay minerals from 1970 to 2018 (Li et al. al., 2019; Zhang et al., 2021). Based on this result, we discuss the change trend of the weathering CS of clay minerals in the past half century. The core calculation formula of the unary linear regression is as follows:

$$\theta = \frac{n \times \sum_{i=1}^{n} (i \times \gamma_i) - \sum_{i=1}^{n} (i) \sum_{i=1}^{n} \gamma_i}{n \times \sum_{i=1}^{n} (i^2) - (\sum_{i=1}^{n} (i))^2} \tag{8}$$

Where, θ is the evolution slope of the CS γ on the pixel, and θ>0 indicates that the CS γ has an overall increasing trend within the current research time limit. i is the current year, n is the overall period of the study, and γi is the value of the CS γ in the i-th year at a certain pixel.

***Separation the effect of SM and STMP***

In order to quantify and distinguish the effects of the two key driving factors, soil moisture and soil temperature, on the CS of the main clay mineral weathering, this paper sets up two independent experiments to simulate the impact of soil moisture changes and soil temperature changes on CS (Liu et al., 2019), in the simulation driven by changes in soil moisture, by limiting the soil temperature, $CO_2$ concentration and the percentage of frozen soil in 1970, and combined with the soil moisture data from 1970 to 2018 year by year, the carbon sink $CS_{(SM)}$ based on soil moisture is estimated, that is, the simulated $CS_{(SM)}$ from 1970 to 2018 is driven by soil moisture. In the same way, the $CS_{(STMP)}$ driven by the soil temperature is simulated.

In order to further analyze the relative contribution of soil moisture/soil temperature/residual factors to the CS of clay minerals, we uses the time as the dependent variable, and use actual CS/the CS driven by SM/the CS driven by STMP as independent variables to do a linear regression analysis to estimate changes in CS under different scenarios. Taking the CS driven by soil moisture ($CS_{(SM)}$) as an example, the calculation formula is as follows:

$$y = \alpha_0 + \alpha_1 t + \tau \tag{9}$$

Among them, y is the CS based on SM simulation with t C km$^{-2}$ ($CS_{(SM)}$); t is the corresponding year, $\alpha_0$ is the intercept, $\alpha_1$ represents the change trend of CS driven by SM ($\Delta CS_{(SM)}$) , τ is the residual error.

In the same way, the actual weathering CS of clay minerals and the change trend of CS driven by soil temperature can be obtained, which are represented by ΔCS and $\Delta CS_{(STMP)}$, respectively. In addition, the change trend of clay mineral weathering CS (ΔRes), which is not driven by the remaining factors explained by soil moisture and soil temperature, is calculated by subtracting the sum of $\Delta CS_{(STMP)}$ and $\Delta CS_{(SM)}$ from the change trend of actual CS ΔCS. Finally, the relative contributions of soil moisture, soil temperature, and remaining factors are calculated by the following formulas:

$$Contr.S.Moi = \frac{|\Delta CS_{SM}|}{|\Delta CS_{SM}| + |\Delta CS_{ST}| + |\Delta CS_{RES}|} \times 100\% \tag{10}$$

$$Con\,tr.S.Tem = \frac{|\Delta CS_{ST}|}{|\Delta CS_{SM}| + |\Delta CS_{ST}| + |\Delta CS_{RES}|} \times 100\,\% \quad (11)$$

$$Con\,tr.S.Res = \frac{|\Delta CS_{RES}|}{|\Delta CS_{SM}| + |\Delta CS_{ST}| + |\Delta CS_{RES}|} \times 100\,\% \quad (12)$$

**Data availability**. All relevant data are available upon request from the authors.

## References


Akselsson, C., Olsson, J., Belyazid, S., Capell, R., 2016. Can increased weathering rates due to future warming compensate for base cation losses following whole-tree harvesting in spruce forests? Biogeochemistry. https://doi.org/10.1007/s10533-016-0196-6

Andrews, J.A., Schlesinger, W.H., 2001. Soil $CO_2$ dynamics, acidification, and chemical weathering in a temperature forest with experimental $CO_2$ enrichment. Global Biogeochem. Cycles 15, 149–162. https://doi.org/10.1029/2000GB001278

Batjes, N.H., Ribeiro, E., Van Oostrum, A., 2020. Standardised soil profile data to support global mapping and modelling (WoSIS snapshot 2019). Earth Syst. Sci. Data. https://doi.org/10.5194/essd-12-299-2020

Beaulieu, E., Goddéris, Y., Labat, D., Roelandt, C., Calmels, D., Gaillardet, J., 2011. Modeling of water-rock interaction in the Mackenzie basin: Competition between sulfuric and carbonic acids. Chem. Geol. https://doi.org/10.1016/j.chemgeo.2011.07.020

Beck, H.E., Zimmermann, N.E., McVicar, T.R., Vergopolan, N., Berg, A., Wood, E.F., 2018. Present and future köppen-geiger climate classification maps at 1-km resolution. Sci. Data. https://doi.org/10.1038/sdata.2018.214

Bibi, I., Icenhower, J., Niazi, N.K., Naz, T., Shahid, M., Bashir, S., 2016. Clay Minerals: Structure, Chemistry, and Significance in Contaminated Environments and Geological $CO_2$ Sequestration, in: Environmental Materials and Waste: Resource Recovery and Pollution Prevention. https://doi.org/10.1016/B978-0-12-803837-6.00021-4

Canarini, A., Kiær, L.P., Dijkstra, F.A., 2017. Soil carbon loss regulated by drought intensity and available substrate: A meta-analysis. Soil Biol. Biochem. https://doi.org/10.1016/j.soilbio.2017.04.020

Charbonnier, G., Duchamp-Alphonse, S., Deconinck, J.F., Adatte, T., Spangenberg, J.E., Colin, C., Föllmi, K.B., 2020. A global palaeoclimatic reconstruction for the Valanginian based on clay mineralogical and geochemical data. Earth-Science Rev. https://doi.org/10.1016/j.earscirev.2020.103092

Chen, H., Bai, X., Li, Y., Li, Q., Wu, L., Chen, F., Li, C., Deng, Y., Xi, H., Ran, C., Luo, X., Liu, M., 2021. Soil drying weakens the positive effect of climate factors on global gross primary production. Ecol. Indic. https://doi.org/10.1016/j.ecolind.2021.107953

Cuozzo, N., Sletten, R.S., Hu, Y., Liu, L., Teng, F.Z., Hagedorn, B., 2020. Silicate weathering in antarctic ice-rich permafrost: Insights using magnesium isotopes. Geochim. Cosmochim. Acta. https://doi.org/10.1016/j.gca.2019.07.031

Dabat, T., Hubert, F., Paineau, E., Launois, P., Laforest, C., Grégoire, B., Dazas, B., Tertre, E., Delville, A., Ferrage, E., 2019. A general orientation distribution function for clay-rich media. Nat. Commun. https://doi.org/10.1038/s41467-019-13401-0

Deng, L., Huang, C., Kim, D.G., Shangguan, Z., Wang, K., Song, X., Peng, C., 2020. Soil GHG fluxes are altered by N deposition: New data indicate lower N stimulation of the $N_2O$ flux and greater stimulation of the calculated C pools. Glob. Chang. Biol. https://doi.org/10.1111/gcb.14970

Deng, Y., Wang, S., Bai, X., Luo, G., Wu, L., Cao, Y., Li, H., Li, C., Yang, Y., Hu, Z., Tian, S., 2020. Variation trend of global soil moisture and its cause analysis. Ecol. Indic. 110, 105939. https://doi.org/10.1016/j.ecolind.2019.105939

Doetterl, S., Berhe, A.A., Arnold, C., Bodé, S., Fiener, P., Finke, P., Fuchslueger, L., Griepentrog, M., Harden, J.W., Nadeu, E., Schnecker, J., Six, J., Trumbore, S., Van Oost, K., Vogel, C., Boeckx, P., 2018. Links among warming, carbon and microbial dynamics mediated by soil mineral weathering. Nat. Geosci. https://doi.org/10.1038/s41561-018-0168-7

Erlandsson Lampa, M., Sverdrup, H.U., Bishop, K.H., Belyazid, S., Ameli, A., J. Köhler, S., 2020. Catchment export of base cations: Improved mineral dissolution kinetics influence the role of water transit time. SOIL. https://doi.org/10.5194/soil-6-231-2020

Erlandsson, M., Oelkers, E.H., Bishop, K., Sverdrup, H., Belyazid, S., Ledesma, J.L.J., Köhler, S.J., 2016. Spatial and temporal variations of base cation release from chemical weathering on a hillslope scale. Chem. Geol. https://doi.org/10.1016/j.chemgeo.2016.08.008

Ferdush, J., Paul, V., 2021. A review on the possible factors influencing soil inorganic carbon under elevated $CO_2$. Catena. https://doi.org/10.1016/j.catena.2021.105434

Flores, B.M., Staal, A., Jakovac, C.C., Hirota, M., Holmgren, M., Oliveira, R.S., 2019. Soil erosion as a resilience drain in disturbed tropical forests. Plant Soil. https://doi.org/10.1007/s11104-019-04097-8

Futter, M.N., Klaminder, J., Lucas, R.W., Laudon, H., Köhler, S.J., 2012. Uncertainty in silicate mineral weathering rate estimates: Source partitioning and policy implications. Environ. Res. Lett. https://doi.org/10.1088/1748-9326/7/2/024025

Goddéris, Y., Brantley, S.L., François, L.M., Schott, J., Pollard, D., Déqué, M., Dury, M., 2013. Rates of consumption of atmospheric $CO_2$ through the weathering of loess during the next 100 yr of climate change. Biogeosciences. https://doi.org/10.5194/bg-10-135-2013

Goddéris, Y., François, L.M., Probst, A., Schott, J., Moncoulon, D., Labat, D., Viville, D., 2006. Modelling weathering processes at the catchment scale: The WITCH numerical model. Geochim. Cosmochim. Acta. https://doi.org/10.1016/j.gca.2005.11.018

Gong, S., Wang, S., Bai, X., Luo, G., Wu, L., Chen, F., Qian, Q., Xiao, J., Zeng, C., 2021. Response of the weathering carbon sink in terrestrial rocks to climate variables and ecological restoration in China. Sci. Total Environ. 750, 141525. https://doi.org/10.1016/j.scitotenv.2020.141525

Hartmann, J., 2009. Bicarbonate-fluxes and $CO_2$-consumption by chemical weathering on the Japanese Archipelago - Application of a multi-lithological model framework. Chem. Geol. https://doi.org/10.1016/j.chemgeo.2009.03.024

Hartmann, J., Moosdorf, N., Lauerwald, R., Hinderer, M., West, A.J., 2014. Global chemical weathering and associated p-release - the role of lithology, temperature and soil properties. Chem. Geol. https://doi.org/10.1016/j.chemgeo.2013.10.025

Ito, A., Wagai, R., 2017. Global distribution of clay-size minerals on land surface for biogeochemical and climatological studies. Sci. Data. https://doi.org/10.1038/sdata.2017.103

Jönsson, C., Warfvinge, P., Sverdrup, H., 1995. Uncertainty in predicting weathering rate and environmental stress factors with the profile model. Water, Air, Soil Pollut. https://doi.org/10.1007/BF00477253

Khan, M.S., Liaqat, U.W., Baik, J., Choi, M., 2018. Stand-alone uncertainty characterization of

GLEAM, GLDAS and MOD16 evapotranspiration products using an extended triple collocation approach. Agric. For. Meteorol. https://doi.org/10.1016/j.agrformet.2018.01.022

Kronnäs, V., Akselsson, C., Belyazid, S., 2019. Dynamic modelling of weathering rates - The benefit over steady-state modelling. SOIL. https://doi.org/10.5194/soil-5-33-2019

Li, H., Wang, S., Bai, X., Cao, Y., Wu, L., 2019. Spatiotemporal evolution of carbon sequestration of limestone weathering in China. Sci. China Earth Sci. https://doi.org/10.1007/s11430-018-9324-2

Li, H., Wang, S., Bai, X., Luo, W., Tang, H., Cao, Y., Wu, L., Chen, F., Li, Q., Zeng, C., Wang, M., 2018. Spatiotemporal distribution and national measurement of the global carbonate carbon sink. Sci. Total Environ. 643, 157–170. https://doi.org/10.1016/j.scitotenv.2018.06.196

Li, Q., Wang, S., Bai, X., Luo, G., Song, X., Tian, Y., Hu, Z., Yang, Y., Tian, S., 2020. Change detection of soil formation rate in space and time based on multi source data and geospatial analysis techniques. Remote Sens. https://doi.org/10.3390/RS12010121

Liu, X., Pei, F., Wen, Y., Li, X., Wang, S., Wu, C., Cai, Y., Wu, J., Chen, J., Feng, K., Liu, J., Hubacek, K., Davis, S.J., Yuan, W., Yu, L., Liu, Z., 2019. Global urban expansion offsets climate-driven increases in terrestrial net primary productivity. Nat. Commun. https://doi.org/10.1038/s41467-019-13462-1

Lynch, J.A., Phelan, J., Pardo, L.H., McDonnell, T.C., Clark, C.M., and Bell, M.D. 2020. Detailed Documentation of the National Critical Load Database (NCLD) for U.S. Critical Loads of Sulfur and Nitrogen, version 3.1, National Atmospheric Deposition Program, Wisconsin State Laboratory of Hygiene, Madison, WI.

Olsson, M., Rosén, K., Melkerud, P.A., 1993. Regional modelling of base cation losses from Swedish forest soils due to whole-tree harvesting. Appl. Geochemistry. https://doi.org/10.1016/S0883-2927(09)80035-8

Pelletier, J.D., Broxton, P.D., Hazenberg, P., Zeng, X., Troch, P.A., Niu, G.Y., Williams, Z., Brunke, M.A., Gochis, D., 2016. A gridded global data set of soil, intact regolith, and sedimentary deposit thicknesses for regional and global land surface modeling. J. Adv. Model. Earth Syst. https://doi.org/10.1002/2015MS000526

Raza, S., Miao, N., Wang, P., Ju, X., Chen, Z., Zhou, J., Kuzyakov, Y., 2020. Dramatic loss of inorganic carbon by nitrogen-induced soil acidification in Chinese croplands. Glob. Chang.

Biol. https://doi.org/10.1111/gcb.15101

Roelandt, C., Godderis, Y., Bonnet, M.P., Sondag, F., 2010. Coupled modeling of biospheric and chemical weathering processes at the continental scale. Global Biogeochem. Cycles. https://doi.org/10.1029/2008GB003420

Romero-Mujalli, G., Hartmann, J., Börker, J., 2018. Temperature and $CO_2$ dependency of global carbonate weathering fluxes – Implications for future carbonate weathering research. Chem. Geol. 1–18. https://doi.org/10.1016/j.chemgeo.2018.08.010

Roy, P.O., Deschênes, L., Margni, M., 2012. Life cycle impact assessment of terrestrial acidification: Modeling spatially explicit soil sensitivity at the global scale. Environ. Sci. Technol. https://doi.org/10.1021/es3013563

Soong, J.L., Castanha, C., Hicks Pries, C.E., Ofiti, N., Porras, R.C., Riley, W.J., Schmidt, M.W.I., Torn, M.S., 2021. Five years of whole-soil warming led to loss of subsoil carbon stocks and increased CO2 efflux. Sci. Adv. https://doi.org/10.1126/sciadv.abd1343

Stocker, T.F., Qin, D., Plattner, G.K., Tignor, M.M.B., Allen, S.K., Boschung, J., Nauels, A., Xia, Y., Bex, V., Midgley, P.M., 2013. Climate change 2013 the physical science basis: Working Group I contribution to the fifth assessment report of the intergovernmental panel on climate change, Climate Change 2013 the Physical Science Basis: Working Group I Contribution to the Fifth Assessment Report of the Intergovernmental Panel on Climate Change. https://doi.org/10.1017/CBO9781107415324

Su, Xueling, Su, Xin, Zhou, G., Du, Z., Yang, S., Ni, M., Qin, H., Huang, Z., Zhou, X., Deng, J., 2020. Drought accelerated recalcitrant carbon loss by changing soil aggregation and microbial communities in a subtropical forest. Soil Biol. Biochem. https://doi.org/10.1016/j.soilbio.2020.107898

Sverdrup, H., Warfvinge, P., 2018. Chapter 11. Estimating field weathering rates using laboratory kinetics, in: Chemical Weathering Rates of Silicate Minerals. https://doi.org/10.1515/9781501509650-013

Sverdrup, H., Warfvinge, P., 1993. Calculating field weathering rates using a mechanistic geochemical model PROFILE. Appl. Geochemistry. https://doi.org/10.1016/0883-2927(93)90042-F

Sverdrup, H.U., Belyazid, S., 2014. Developing an approach for Sweden, Switzerland, United

States and France for setting critical loads based on biodiversity including management, pollution and climate change. Ecol. Modell. https://doi.org/10.1016/j.ecolmodel.2014.09.020

Whitfield, C.J., Phelan, J.N., Buckley, J., Clark, C.M., Guthrie, S., Lynch, J.A., 2018. Estimating base cation weathering rates in the USA: Challenges of uncertain soil mineralogy and specific surface area with applications of the profile model. Water. Air. Soil Pollut. https://doi.org/10.1007/s11270-018-3691-7

Xi, H., Wang, S., Bai, X., Tang, H., Luo, G., Li, H., Wu, L., Li, C., Chen, H., Ran, C., Luo, X., 2021. Science of the Total Environment The responses of weathering carbon sink to eco-hydrological processes in global rocks. Sci. Total Environ. 788, 147706. https://doi.org/10.1016/j.scitotenv.2021.147706

Yu, Z., Chen, H.Y.H., Searle, E.B., Sardans, J., Ciais, P., Peñuelas, J., Huang, Z., 2020. Whole soil acidification and base cation reduction across subtropical China. Geoderma. https://doi.org/10.1016/j.geoderma.2019.114107

Zeng, S., Liu, Z., Kaufmann, G., 2019. Sensitivity of the global carbonate weathering carbon-sink flux to climate and land-use changes. Nat. Commun. https://doi.org/10.1038/s41467-019-13772-4

Zhang, S., Bai, X., Zhao, C., Tan, Q., Luo, G., Wang, J., Li, Q., Wu, L., Chen, F., Li, C., Deng, Y., Yang, Y., Xi, H., 2021. Global $CO_2$ Consumption by Silicate Rock Chemical Weathering: Its Past and Future. Earth's Futur. https://doi.org/10.1029/2020EF001938

Zhao, W., Zhang, R., Cao, H., Tan, W., 2019. Factor contribution to soil organic and inorganic carbon accumulation in the Loess Plateau: Structural equation modeling. Geoderma. https://doi.org/10.1016/j.geoderma.2019.06.005

Zhu, Y., Liu, •Yi, Wang, W., Singh, V.P., Ren, L., 2021. A global perspective on the probability of propagation of drought: From meteorological to soil moisture. J. Hydrol. https://doi.org/10.1016/j.jhydrol.2021.126907

Zolkos, S., Tank, S.E., Kokelj, S. V., 2018. Mineral Weathering and the Permafrost Carbon-Climate Feedback. Geophys. Res. Lett. https://doi.org/10.1029/2018GL078748

# Supplementary Files

This is a list of supplementary files associated with this preprint. Click to download.

- Supplementarymaterial.doc